Proceedings of the 2009 IEEE International Conference on Systems, Man, and Cybernetics
San Antonio, TX, USA - October 2009

MR-Damper based Control System

Jorge Lozoya-Santos*, Ruben Morales-Menendez†, Ricardo Ramirez-Mendoza‡,
*PhD Student, †Associate Director of Research, ‡Director of the CIDyT
Tecnológico de Monterrey, Campus Monterrey
Monterrey NL, México 64849
{jorge.lozoya, rmm, ricardo.ramirez}@itesm.mx

***Abstract*—The precise variation of the magneto-rhelogical (*MR*) damping force in a semi-active suspension is a key issue in order to assure the desired performances over a suspension control system. The open loop control of this force is a very common strategy. Other schemes propose adaptive controller alternatives while the automotive hardware is a constrained computation resource. This paper proposes the implementation of the damping force control system based on the *MR* damper using an internal model control approach. The controller and the internal model are proposed as artificial neural networks (*ANN*) trained and validated with realistic automotive datasets. The results shows good servo control and fast regulation to abrupt disturbances without on-line *ANN* tuning computations.**

***Index Terms*—*MR*-Damper, Control System, Internal Model Control, Artificial Neural Network**

I. INTRODUCTION

A damper that uses a Magneto-Rheological (*MR*) fluid, oil with metallic particles, having the feature of the variation of its damping ratio is named a semi-active *MR* damper. The main function of the *MR* damper in an automotive suspension is to absorb energy in order to get low accelerations of the sprung mass (i.e. automotive chassis) and safety deflections between sprung and unsprung masses.

The variation of the damping ratio in a *MR* damper is done by manipulating the electric current supply through a coil. The coil is located inside the *MR* damper cylinder, in the area of the oil flow. Therefore, if the electric current is increased, the viscosity of the oil is increased too. The viscosity is directly proportional to the force that the *MR* damper delivers to the suspension. The force is affected in a non-linear way by the velocity deflection in the suspension. Thus the non-linearity of this system makes the semi-active suspension control a challenging task.

Into the semi-active suspension control system, the electric current (manipulation) must be determined by the controller looking for a desired damping force. The *MR* damper model plays a key role in this control strategy performance; specially for a model based controller.

The delivered *MR* damper force is an over-damped response when the coil has a stepped increment in the supplied electric current with a constant velocity in the vertical axis. The displacement of the *MR* damper becomes non-linear due to the velocity variations. The non-linearity at different frequencies plus a high hysteresis represent a complex behavior. Therefore, modelling a *MR* damper is not a trivial task.

This paper proposes the implementation of the damping force control system based on the *MR* damper using the Internal Model Control (*IMC*) approach. The paper organization is structured as follows: section II reviews the background; section III exposes internal model control concepts using artificial neural networks (*ANN*); the implementation details of the controller, the servocontrol and regulatory control tests are presented in section IV. The results over *ANN* modelling for the inverse and forward *MR* damper models and the validation of the control approaches are shown in Section V. The section VI concludes the paper.

TABLE I
NOMENCLATURE

Variable	Description
x	MR damper piston displacement
$\dot{x}$	MR damper piston velocity
$\hat{F}_{MR}$	MR damper force
a_1	Yield F_{MR} coefficient
a_2	Post-yield F_{MR} coefficient
a_3	Pre-yield F_{MR} coefficient
a_4	Absolute value of hysteretical critical $\dot{x}(i)$
a_5	Absolute value of hysteretical critical $x(i)$
I_{MR}	Electrical current exciting MR damper
$\hat{I}_{MR}$	Estimated Electrical current to excite MR damper
$F_{MR}sp$	Reference force in feedback loop
F_{MR}	Measured Force in feedback loop
d'	Disturbance

II. BACKGROUND

A full semi-active suspension control algorithm computes the desired force in order to minimize the acceleration of the mass sprung acting on the comfort and the deflection between sprung and unsprung masses acting on the road holding on the specified ranges. This work is performed directly over the deflection through a *MR* damping force (Fig. 1).

The variables in the control of the *MR* damper force are the electric current as manipulation, the displacement of the *MR* damper piston generated by the road as the main disturbance and the generated damper force as the controlled variable. The generic features of this control system are:

1) The road is the source of non-linearity; it can be estimated through an accelerometer.
2) If high frequency displacement appears, the non-linearity will act on controller performance.
3) The best road holding and comfort regulation depend on the *MR* damper model.
4) The electric current through the *MR* damper coil is controlled by a I-driver.

978-1-4244-2794-9/09/$25.00 ©2009 IEEE

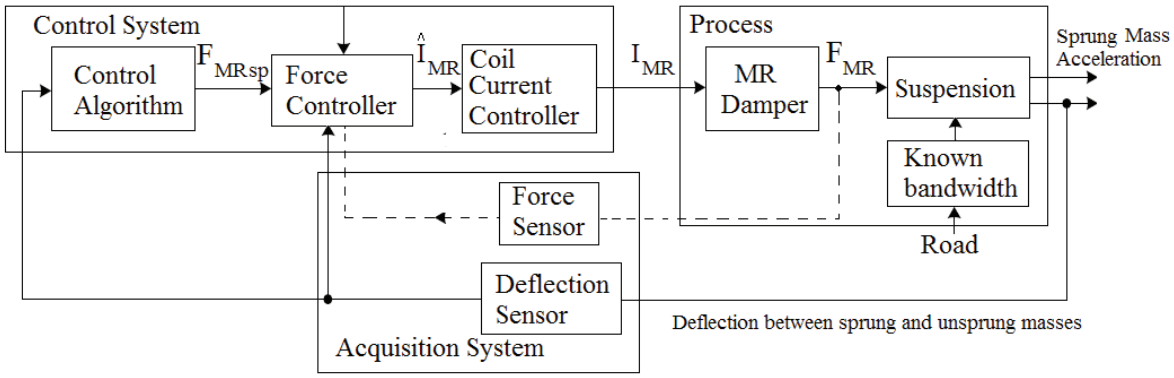

Fig. 1. Standard control for a semi-active suspension. The road is the main disturbance of a known bandwidth.

5) The force controller needs to be non-linear.

The force controller plays a crucial role inside the full suspension control system. A precise *MR* damper model improves significantly the force controller performance. A *MR* damper model relates the electric current, displacement or velocity of the *MR* damper piston as inputs and the *MR* damper force as output.

A *MR* damper can be modeled as: phenomenological [1], semi-phenomenological [2], black-box (*ANN* based) [3], [4], [5] and statistical approaches [6]. The model parameters can be identified using recursive least square algorithm except for: the phenomenological model (modified Bouc Wen model) which implies a more complex identification, and the statistical models using the surface response method.

The control system for the *MR* damping force has been implemented in open loop and feedback control.

The open loop control is performed via an inverse model of the *MR* damper placed in series with the *MR* damper, as it can be seen in the Figure 1, where the force controller are placed in series with the coil current controller and the *MR* damper, without the force sensor. The controller computes the electrical current needed to obtain the force. If a disturbance acts on the controlled force, the outer control loop has to act in order to avoid the deviation from nominal performance. The coverage of the semi-active plane displacement versus desired force is not assured and the bandwidth of manipulation could be unreal for some setpoints [7],[8],[9].

The feedback control of the *MR* damper force has an intrinsic robustness and it produces feasible manipulations. The feedback is performed via a force sensor, see Figure 1, dotted line. Typically, the controller parameters must be updated every sampling time in order to adapt the controller to uncertainties and process variations. Some artificial intelligence techniques such as neuro-fuzzy and genetic algorithms have been tried. The main drawback of these approaches are specialized hardware and computation capability needed [10], [11], [12], [13]. Table II summarizes representative research works where the lack of a control system with light-computation algorithms, optimum performance and high utilization of the semi-active zone is evident.

TABLE II
REPRESENTATIVE WORKS. OL IS OPEN LOOP CONTROL, FL IS FEEDBACK LOOP CONTROL.

Autor	Advantage	Drawback	Comments
[14, Kim 1999, OL]	Linear control theory can be applied	Wasted zones in actuatorś domain	Linearization of *MR* damper
[7, Li 2006, OL]	Good tracking of *MR* damping force	Unfeasible manipulation bandwidth	- Constrained I as targets - It uses an inverse *ANN* model
[8, Wang 2005, OL], [9, Xia 2003, OL]	Good tracking of *MR* damping force	Not evidence on disturbance rejection	- Elimination of the force sensor - It uses an inverse *ANN* model
[10, Xu2003, FL]	Control of suspension deflection	Low action bandwidth $\leq 6Hz$ with time delay	- On-line real-time learning and control - AI + ANN controller
[11, Fu 2005, FL]	Lyapunov function based	On-line ANN tunning	- %10 acceleration reduction - AI + Neuro-Fuzzy adaptive
[12, Karkoub 2006, FL]	Simple Implementation	Constrained semi-active zone	Fuzzy control
[13, Mori 2007, FL]	Good tracking control inverse model	- On-line computations for forward, inverse and two adaptive algorithms	Slow convergence - IMC Adaptive controller

III. *IMC*-BASED CONTROL SYSTEM

The *IMC* strategy is a feedback loop control where an internal model (*M*) is added in parallel with the process (*P*), Fig. 2. The controlled variable (F_{MR}) is compared with the internal model output ($\hat{F}_{MR}$). The difference between the F_{MR} and $\hat{F}_{MR}$ is the feedback signal. The later is the estimation of disturbances over the process; the accuracy of this estimation is pending of model fidelity [15]. The subtract $F_{MR} - \hat{F}_{MR}$ is also subtracted from the feedback loop setpoint ($F_{MR}setpoint$) and this feeds a filter (F). The function of F is to diminish the noise over the manipulation ($\hat{I}_{MR}$). Finally the controller (C), using the error filtered $F'_{MR}setpoint$,

computes $\hat{I}_{MR}$.

In this approach, the model of the process and the controller are an *ANN* forward ($M = ANN_{FWD}$) and an *ANN* inverse ($C = ANN_{INV}$) model of the *MR* damper respectively [16], Fig. 2.

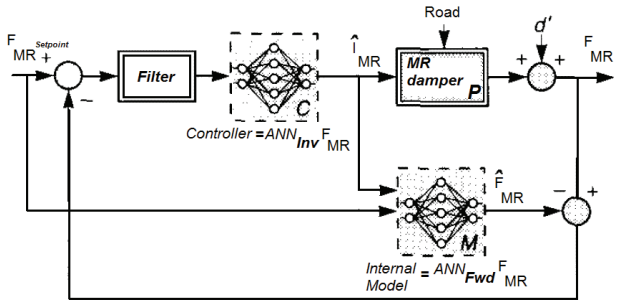

Fig. 2. *IMC* with *ANN* (modified from [16]). The process is the *MR* damper. The internal model receives the history of the desired force and the controller output.

If the ANN_{FWD} is perfect (i.e $ANN_{FWD} = Process$) then closed loop system is stable, if and only if the controller and the process are open loop stable. Under the assumption such that the right inverse of the ANN_{FWD} dynamics exists and if the controller is equal to the ANN_{INV} ($Controller = ANN_{INV}$) and the close loop is stable, then a perfect control is achieved for any $road$; therefore, if the static gain of the controller is equal to the inverse of the model gain, ($Controller_K = ANN^{-1}_{FWD}$), where the subscript K denotes steady state hence asymptotically the following error will be zero.

It is important to remark that the *IMC* structure demands the inverse model trained with the experimental data set to assure the free error response in steady state.

A system can be modelled as finite impulse response (*FIR*) if it is stable and its impulse response is reasonably fast [17]. The dynamics response of the *MR* damping force regarding to electric current is an over-damped response, then its impulse response is reasonably fast and it is stable [18]. Hence, an inverse ANN_{INV} with inputs structured like those for finite impulse response models is feasible.

For the internal model, the ANN_{FWD} model with inputs structured like those for auto-regressive with exogenous models is used. Fig. 3 shows the *ANN* architectures for both models where x_i represents the i-esime displacement, I_i represents the i-esime electric current and f_{MR_i} represents the i-esime *MR* damper force.

IV. Implementations

Several experiments were developed in an industrial laboratory located at *Metalsa*[1]. Figure 4 shows the main components of experimental setup. The shown components are: ACDelco^{TM} *MR* damper and a MTS^{TM} system (3,000 psi

[1]www.metalsa.com.mx

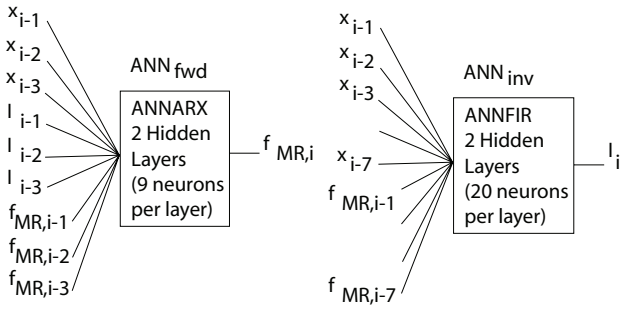

Fig. 3. *ANN* architectures for *IMC* strategy application. ANN_{fwd} needs displacement, electric current and damping force and their past values for actual damping force prediction. ANN_{inv} needs displacement and damping force for electric current prediction.

actuator, MTS^{TM} controller GT and a MTS^{TM} FlexTest software). The sample frequency was 512 Hz in th data acquisition system.

The experimental databases were generated based on a classic Design of Experiments (*DoE*), using sinusoidal displacement with fixed frequency at 30 cycles and a constant electric current. The operating conditions of the *MR* damper were stroke: $0 - 0.025$ m, displacement bandwidth: $0.5 - 14.5$ Hz, electric current: $0 - 4$ A. The increments on current and frequency displacement were: 0.25 A per each complete displacement bandwidth and 0.5 Hz. The measured force had a range $0 - 2850$ N.

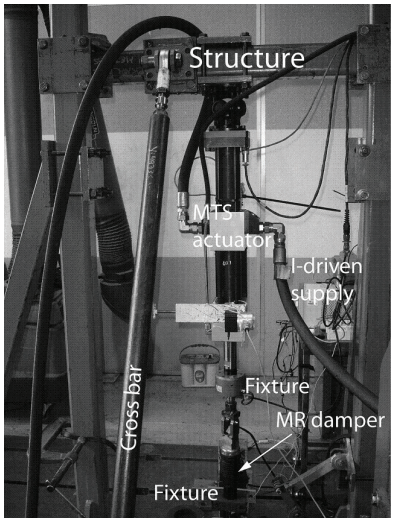

Fig. 4. Experimental setup. The structure is fixed with a cross bar. The specimen has fixtures at three points: top, middle and bottom. The actuation is done over top of the *MR* damper. The I-driver controls the coil electric current. The displacement is measured with a sensor inside the actuator. The force is measured between the actuator and the top fixture.

Each database consists of a road and electric current sequences. These database were applied to the *MR* damper in order to obtain the generated force. Each pattern consists of three *measured* sequences of data sampled at 512 Hz: displace-

ment (x), electric current (I), and delivered *MR* damper force (F_{MR}).

A *MR* damper model based on a semi-phenomenological equation (1) was identified with these experimental patterns.

$$\hat{F}_{MR} = a_1 tanh[a_3(\dot{x} + \frac{a_4}{a_5}x)] + a_2[\dot{x} + \frac{a_4}{a_5}x] \qquad (1)$$

The coefficients of model (1) were represented as a polynomial function of electric current value. The adopted fitting process was recursive least squares with parameter adaptation [19]. The model performance for several currents was very good. This model reproduces the hysteretic behavior with high accuracy.

Given a database, two datasets were generated for the training and testing procedure of both ANN_{FWD} and ANN_{INV}. The databases consist of a Smooth Highway (*SH*) road profile [20], and an Increased Clock Period Signal (*ICPS*) [21] for the electric current (Fig. 5).

For the *IMC* based control system evaluation, eight realistic databases were proposed. For road profiles were: Smooth Highway (*SH*), Rough Runway (*RR*), Smooth Runway (*SR*), *SR* with white Noise of % 10 (*SRN*), *SR* with white noise of % 20 (*SRN2*) and Pasture Road (*PS*). Each aforementioned sequence was generated by different seed. Every sequence was added with a % 5 white noise amplitude. A pseudo-random binary sequence (*PRBS*) was generated for each road profiles as electric current. The *PRBS* minimum step duration was $1/30$ seconds (Fig 5).

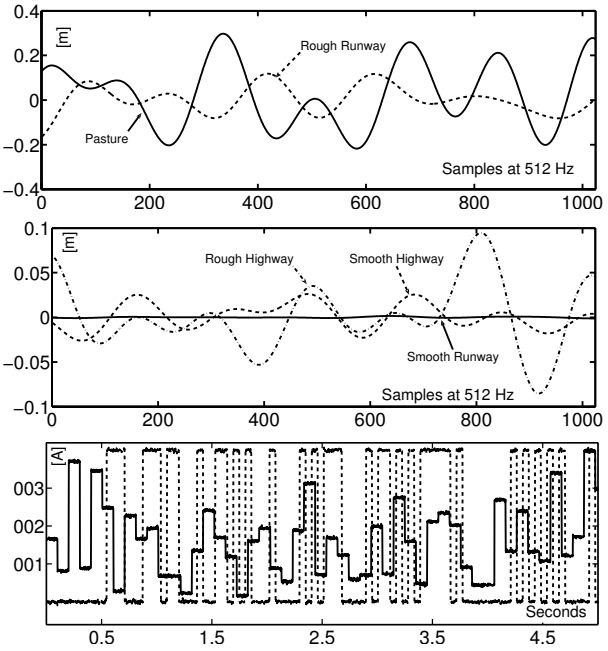

Fig. 5. Design of Experiments. Top and middle plot shows a detail of the road profiles; while the bottom plot shows the kind of electric current signals: PRBS and ICPS.

The *IMC* with *ANN* was implemented according to Fig. 2. The operator $Filter$ was a first order system. The time constant was computed based in spectral density of error between a open loop control force and the ANN_{FWD} model. The *MR* damper was simulated with the model (1). The $road$ was the deflection of *MR* damper piston and the Fsp_{MR} was the force corresponding to simulated pattern. The disturbance was a constant stepped force added at the output system. In order to bound the actuation, a saturation operator between $0-4$ A was placed at the controller output.

The $Error-to-Signal-Ratio$ (*ESR*) is used as quality tracking force index [5]. The *ESR* is the ratio between the sum of square errors and the variance of the output.

$$ESR = \frac{\sum_{i=1}^{N}(F_{MRi} - \hat{F}_{MRi})^2/N}{Var_{F_{MR}}} \qquad (2)$$

where F_{MRi} is the real force, $\hat{F}_{MRi}$ is the tracked force estimation, N is the number of samples, and $Var_{F_{MR}}$ is the variance of the real force.

The controller was widely validated under two approaches: Servo-Control (Tracking) and Regulation. The Servo-Control approach consisted of exposing controller to several test patterns creating realistic automotive scenarios: a road profile in the displacement and a *PRBS* electric current. The regulation approach was tested adding a step disturbance at the system output when the controller was working into the aforementioned scenarios. The ANN_{FWD} and ANN_{INV} did not change through evaluation.

V. RESULTS

A. *Inverse and Forward* ANN *Models*

The ANN_{FWD} and ANN_{INV} models were tested with several input signals, Table III. The *ANN* models shows an accurate identification. The ANN_{INV} model was not as good as ANN_{FWD}, the *ESR* for each signal was low and almost constant. The higher *ESR* for ANN_{INV} model was in the patterns *SR*, *SRN* and *SRN2*. This is because the maximum displacement in these patterns are very small in relation with the training domain, and the magnitude of the noise. In consequence the ANN_{INV} can not to asses the difference between signal and noise. All the *ESR* for the ANN_{FWD} model were very low except for *SRN*.

TABLE III
MODELLING PERFORMANCE.

Testing Pattern	ANN_{fwd}	ANN_{inv}
Smooth Highway	8^{-8}	0.1257
Rough Runway	7^{-7}	0.0512
Smooth Runway	1^{-5}	0.6056
Smooth Runway with Noise % 10	0.052	1.72
Smooth Runway with Noise % 20	8^{-5}	1.7
Pasture Road	2^{-7}	0.5628

Left plot in Fig. 6 shows a box and whisker plot where ANN_{FWD} model is a good approximation, no matter inputs signal. In this box and whisker plot there is a box for each model that compares the *ESR*. The boxes have lines at the

lower quartile, median, and upper quartile values. The whiskers are lines extending from each end of the boxes to show the extent of the rest of the data. Outliers are data with values beyond the ends of the whiskers. ANN_{INV} model exhibits higher variability compared with ANN_{FWD} model.

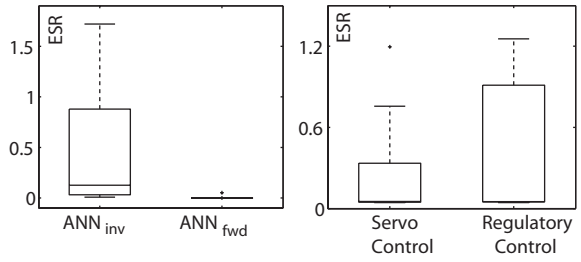

Fig. 6. Boxplots for modelling and controller tests. Each boxplot is based on the results from the tables III and IV.

B. Servo-Control Approach Performance

The *IMC* based control strategy was implemented by substituting directly the ANN_{FWD} and ANN_{INV} as the internal model and controller respectively.

Table IV shows that *ESR* for servo-control approach are always under 6%, except for the *SRN* and *SRN2* inputs where the *ESR* are higher. When the *SR* is fed through the system offers an $ESR = 20\%$, considering that ANN_{INV} model is not good; it could be an acceptable value. Using the pasture road profile, which maximum displacement was 0.1 m, shows also a good force servo-control.

In one side, for the tested patterns, the controller follows the F_{MR} setpoint.

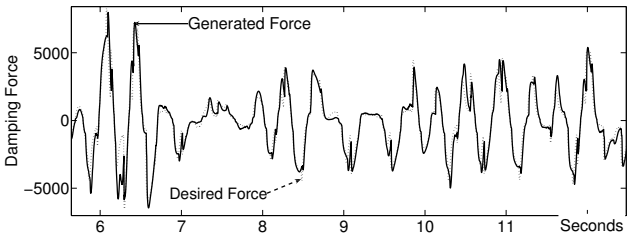

Fig. 7. Servo-control Performance for pasture road profile.

In other side, a tracking error on the *MR* damping force was seen for each pattern tested, see figures 7 and 8 top plot. This could be due to the probability of the backpropagation algorithm to stand in a local minimum instead of the global minimum [22]. It is shown by the ESRs in Table III that the ANN_{INV} is not enough closer to the general inverse process. Hence, there is a research opportunity in order to obtain *MR* ANN_{INV} model.

The results obtained show that although the controller is not adaptive, when it is submitted to a test patterns with higher amplitudes in road and force (desired by the control suspension system) respectively, the tracking of the *MR* damping force is succeeded.

C. Regulatory Control Approach Performance

The disturbance d' consisted of an addition of 100 Newtons on the output of the close loop at 10^{th} sec and a subtraction of 50 Newtons at 20^{th} sec. This disturbance is acting on the output of the closed loop system (Fig. 2).

The column *Regulatory Control* in Table IV and Fig. 6 right side second column shows the results.

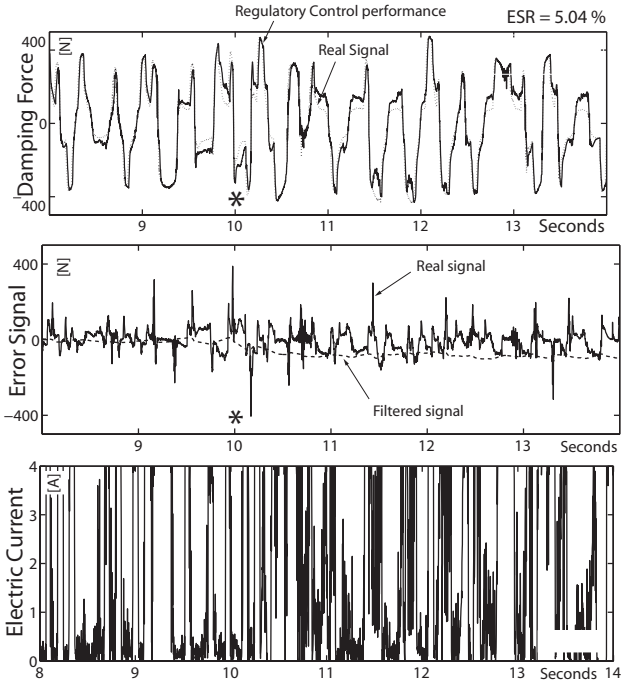

Fig. 8. Regulatory Control Performance.

The *IMC* based strategy diminished the effect of the step disturbance on the system. The *ESR* increased substantially for *SR*, *SRN* and *SRN2*.

Fig. 8 shows some results when the control system is tested with a *Smooth Highway* profile. Top plot shows the damping force, middle plot shows the error between *MR* damper and ANN_{FWD} model before and after filtering; finally, bottom plot shows the PRBS electric current manipulation. The error signal at 10 sec (* symbol) shows a deviation; however, the

TABLE IV
PERFORMANCE OF CONTROL SYSTEM APPROACHES.

Testing Pattern	*ServoControl Approach*	*Regulatory Approach*
Smooth Highway	0.0448	0.0504
Rough Runway	0.0519	0.0518
Smooth Runway	0.1943	0.8132
Smooth Runway with Noise % 10	1.1961	1.207
Smooth Runway with Noise % 20	0.7565	1.255
Pasture Road	0.0847	0.0851

force tracking did not suffer a important negative effect. Then, *IMC* strategy rejects disturbances.

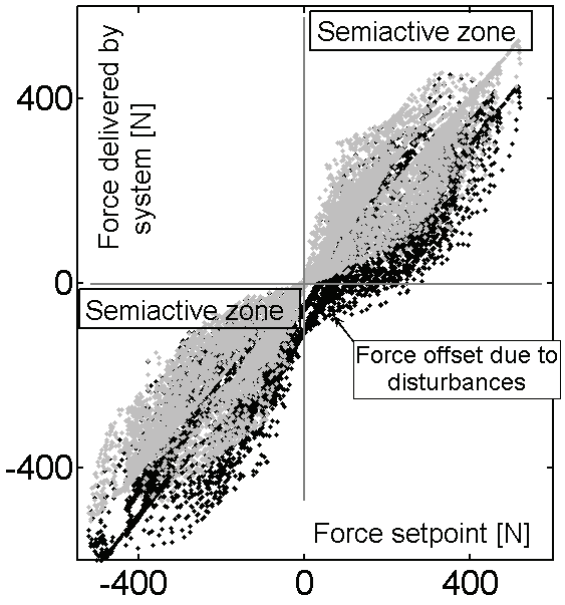

Fig. 9. Force commanded versus force delivered. The black dots are the force generated by open loop control. The grey dots are those correspondent for the *IMC* control under the same disturbance.

Figure 9 shows the commanded force versus delivered force under the regulatory control approach for the *Smooth Highway* profile. The IMC based feedback control delivers the *MR* damping force (grey dots) in order to get good performance; while, an open loop (dark dots) does not have a right compensation for disturbance invading not semi-active force zones. The disturbance rejection is complete and the force delivered to system stands on the semi-active zones.

The not adaptive proposed controller has not the drawback of computing the Hessian of the weight matrix at each updating. The convergence speed will affect the control suspension performance, hence a convergence time bigger than 1 second [13] is not convenient in automotive application.

VI. CONCLUSIONS

A not adaptive *IMC* based control strategy was tested in order to control *MR* damper force into a semi-active suspension control system. The results show good servo control, fast regulation response to abrupt disturbances, and realistic manipulations.

The application of realistic data sets as road profiles and PRBS electric current signals with white noise were a key step into the identification procedure of the *MR* damper models.

Also these datasets allows to validate that while an adaptive scheme could need of high convergence speed, hence high computation capability resources, the proposed approach controls the *MR* damper force with a static controller based on good identification of the device.

REFERENCES

[1] B. Spencer, S. Dyke, M. Sain, and J. Carlson, "Phenomenological Model of a MR Damper," *ASCE Journal of Engineering Mechanics*, vol. 123, pp. 230–238, 1996.

[2] S. Guo, S. Yang, and C. Pan, "Dynamical Modeling of Magneto-rheological Damper Behaviors," *Intelligent Material Systems and Structures*, vol. 17, pp. 3–14, 2006.

[3] G. Jin, M. K. Sain, and B. E. S. Jr., "Nonlinear Blackbox Modeling of MR-dampers for Civil Structural Control," *Control Systems Technology, IEEE Transactions on*, vol. 13, no. 3, pp. 345–355, 2005.

[4] S. B. Choi, S. K. Lee, and Y. P. Park, "A Hysteresis Model for Field-Dependent Damping Force of a Magnetorheological Damper," *Journal of Sound and Vibration*, vol. 245(2), p. 375383., 2001.

[5] S. M. Savaresi, S. Bittanti, and M. Montiglio, "Identification of Semi-Physical and Black-Box Non-linear Models: the Case of MR-dampers for Vehicles Control," *Automatica,*, vol. 41, no. 1, pp. 113–127, 1 2005.

[6] A. C. Shivaram and K. V. Gangadharan, "Statistical Modeling of a Magneto-rheological Fluid Damper using the Design of Experiments Approach," *Smart Materials and Structures*, vol. 16, no. 4, pp. 1310–1314, 2007.

[7] Z. Li, J. Liu, and Y. He, "Intelligent control and tracking identification of magnetorheological damper based on improved bp neural networks," in *Intelligent Control and Automation, 2006. WCICA 2006. The Sixth World Congress on*, vol. 1, 2006, pp. 1901–1905.

[8] D. H. Wang and W. H. Liao, "Modeling and Control of Magnetorheological Fluid Dampers using Neural Networks," *Smart Mater. Struct.*, vol. 14, pp. 111–126, 2005.

[9] P.-Q. Xia, "An Inverse Model of MR Damper using Optimal Neural Network and System Identification," *Journal of Sound and Vibration*, vol. 266, no. 5, pp. 1009–1023, 10/2 2003.

[10] Z.-D. Xu, Y.-P. Shen, and Y.-Q. Guo, "Semi-active Control of Structures Incorporated with Magnetorheological Dampers using Neural Networks," *Smart Mater. Struct.*, vol. 12, pp. 80–87, 2003.

[11] L. J. Fu, J.G.Cao, C. R. Liao, and B. Chen, "Study on Neural Networks Control Algorithms for Automotive Adaptive Suspension Systems," in *Neural Networks and Brain, 2005. ICNN&B '05. International Conference on*, 2005.

[12] M. Karkoub and M. Zribiz, "Active/Semi-active Suspension Control using Magnetorheological Actuators," *Int. J.of Sys. Sci.*, vol. 37-1, pp. 35–44, 2006.

[13] T. Mori, I. Nilkhamhang, and A. Sano, "Adaptive Semi-active Vibration Isolation Considering Uncertainties of MR Damper and Suspension Structure," in *Proceedings of the 46th IEEE Conference on Decision and Control, New Orleans, LA, USA, Dec. 12-14.*, 2007.

[14] B. Kim and P. N. Roschke, "Linearization of Magnetorheological Behavior using a Neural Network," in *Proc. of the American Ctrl. Conf. San Diego, California*, 1999.

[15] M. Morari and E. Zafiriou, *Robust Process Control*. Prentice Hall, 1989.

[16] K. Hunt and D. Sbarbaro, "Neural Networks for Nonlinear Internal Model Control," *Control Theory and Applications, IEE Proceedings D [see also IEE Proceedings-Control Theory and Applications]*, vol. 138, no. 5, pp. 431–438, 1991, iMC.

[17] L. Ljung, *System Identification : Theory for the User*. Prentice Hall PTR, 1999.

[18] J.-H. Koo, F. D. Goncalves, and M. Ahmadian, "A Comprehensive Analysis of the Response Time of MR Dampers," *Smart Mater. Struct.*, vol. 15, pp. 351–358, 2006.

[19] Y. D. Landau, R. Lozano, and M. M'Saad, *Adaptive Control*. Springer Verlag, 1998.

[20] S. Park, A. Popov, and D. Cole, "Influence of Soil Deformation on Off-road Heavy Vehicle Suspension Vibration," *Journal of Terramechanics*, vol. 41, pp. 41–68, 2004.

[21] T. Soederstrom and P. Stoica, *System Identification*. Prentice Hall, 1989.

[22] M. T. Hagan, "Training feedforward networks with the marquardt algorithm," pp. 989–993, 1994, iD: 1.